JOURNAL OF THEORETICAL
AND APPLIED MECHANICS
3, 40, 2002

ANALYTICAL MODELLING OF ELECTRORHEOLOGICAL MATERIAL BASED ADAPTIVE SHELLS

ANDRZEJ TYLIKOWSKI

Institute of Machine Design Fundamentals, Warsaw University of Technology
aty@simr.pw.edu.pl

Electrorheological fluids show immediate variations of their rheological properties when subjected to varying electric fields. This study presents vibration analysis of a closed cylindrical shell partially filled with controllable fluids. The analysed structure as an element of harmonic drive can generate torsional vibration due to the wave generator operation. As a result of the study, fluid-filled laminated cylindrical shell has shown an increased and controllable damping capacity as compared to the conventional shell.

Key words: shell torsional vibrations, electrorheological fluid, dynamic characteristics

1. Introduction

Electrorheological materials are suspensions of dielectric particles in nonpolar liquids that exhibit dramatic changes in rheological sesponse when exposed to an electric field (Shiang and Coulter, 1996). The rheological changes are fast (10^{-3} s) and reversible, thereby making the fluids suitable to real-time control of vibration. The controllable materials are usually modelled as the Bingham viscoelastic materials. The fluid is very versatile in that it connects properties of solids and liquids. The controllable rheological behaviour of electrorheological materials is useful in engineering systems and structures, where variable performance is desired. As a result we can obtain an intelligent or an adaptive structure, which reacts in an appropriate manner so as to meet the defined performance criteria, eg. minimizing vibrational amplitude or damping its response (Choi et al., 1992). The crucial point in developing an adaptive structure is to create a mathematical model of the dynamic structural

response. Electrorheological-based beam structures in a shear configuration were modelled in the past as a modified Bernoulli-Euler beam (Ross et al., 1959) and as a sixth-order partial differential equation (Mead and Markus, 1969). The symmetrically laminated structure consisting of the uniform beam and the multi-cell chains containing the electrorheological fluid in an extensional configuration was analysed (Tylikowski, 2000) using the Oldroyd equation (Oldroyd, 1953). Treating the beam as a moderately thick plate with the rotary inertia term, it was shown that the electric activation increases the stiffness and the damping property described by a retardation time of the adaptive beam.

The harmonic drive is a special speed reduction system, whose operation principle is based on elastic deformations. The harmonic drive is composed of a rigid circular ring, oval wave generator and flexible cylindrical shell, which is called the flexpline. From the components of harmonic drive, the cylindrical shell is the main element for the transmision of motion. It has to be flexible in the radial direction, and must be stiff in the torsional direction to transmit rotational motion. It should also dissipate the transient short-lived torsional vibration. It is shown (Han Su Jeon, 1999) that the use of composite or hybrid flexplines increases significantly the damping ratio and improves the quality as compared to the conventional steel flexpline.

This study presents vibration analysis of a closed cylindrical shell partially filled with the controllable fluids. As a result of the study, fluid-filled laminated cylindrical shell has shown an increased and controllable damping capacity as compared to the conventional shell.

2. Dynamic shell equations

Consider the elastic closed cylindrical shell with the radius R, length ℓ, thickness h. A torsional motion is described by the circumferential displacement v. The viscous model of material damping with the coefficient λ is assumed to describe the dissipation of the shell energy. The internal damping effect will be taken into account in the final form, using an elastic-viscoelastic correspondence principle. It the present approach, radial and longitudinal shell displacements are neglected. Due to the geometry, the shell is divided into three parts as shown in Fig. 1, and the dynamic behavior of each part will be described separately.

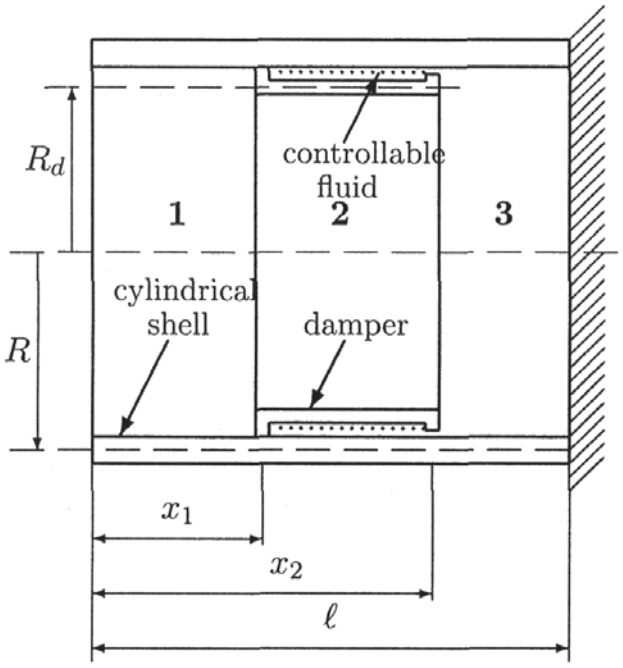

Fig. 1. Cylindrical shell with controllable fluid-filled distributed fixed-free damper

The torsional vibrations of elastic shell in the ith section are described by the classical wave equation of the form

$$Gh(1+\beta^2)v_{i,xx} - \rho h v_{i,tt} = q_v \qquad x \in \{x_{i-1}, x_i\} \tag{2.1}$$

where $i = 1,2,3$, $x_0 = 0$, $x_3 = l$, G is the Kirchhoff modulus and $\beta^2 = h^2/(12R^2)$ is the geometric parameter. Inside the main shell structure, the closed cylindrical shell is axisymmetrically mounted in the second section in such a way that the space between the shells is filled by the controllable fluid and both the annular ends are sealed. An electric field applied to the electrorheological material has the radial direction. The polarization of the ER suspension leads to configuration changes, which in turn result in significant changes in rheological properties. They are described by a tangential loading in the circumferential direction. Analysing a controllable fluid operation, we have the direct shear mode in the circumferential direction. The external loading is denoted by q_v. In the first and the third section the external loading is equal to zero. In the second section, the external loading is equal to the shear stress

$$q_v = -\tau = K\frac{v_2 - v_d}{\delta} \tag{2.2}$$

where K is the stiffness of the active material placed in the gap between the external and internal shell, δ is the thickness of active material. Dynamics of

the inner shell (damper) is described by the equation of the form

$$G_d h_d(1+\beta_d^2)v_{d,xx} - \rho_d h_d v_{d,tt} = \tau \qquad x \in \{x_1, x_2\} \tag{2.3}$$

Two configurations of the ER damper will be analysed. In the first configuration the inner shell is connected with the main shell by means of a rigid ring at $x = x_1$. Therefore, at the left-hand edge $x = x_1$, the damper circumferential displacement and the main shell circumferential displacement are equal. The right-hand end of the damper $(x = x_2)$ is free.

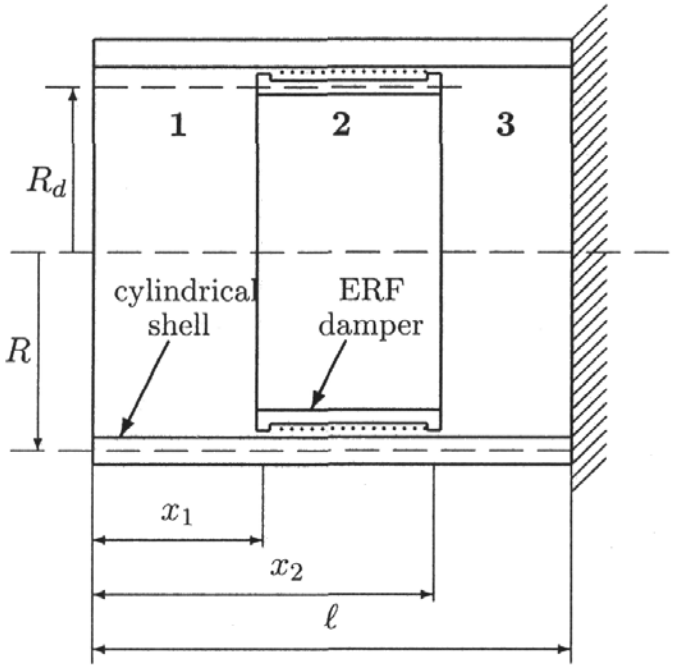

Fig. 2. Cylindrical shell with controllable fluid-filled distributed free-free damper

The second configuration corresponds to the case of both ends free. It is assumed that the torques carried by the rubber sealing at the ends of damper are negligible.

3. Boundary conditions

The shell in both configurations is fixed

$$v_1(t,0) = 0 \tag{3.1}$$

at the end $x = 0$, and loaded by external harmonic torque at $x = \ell$

$$M = 2\pi h R^2 \tau(t,\ell) = 2\pi h R^2 G v_{3,x}(t,\ell)\mathrm{e}^{\mathrm{i}\omega t} \tag{3.2}$$

The conditions at $x = x_1$ and $x = x_2$ represent the continuity of displacements

$$\begin{aligned} v_1(t, x_1) &= v_2(t, x_1) \\ v_1(t, x_1) &= v_d(t, x_1) \\ v_2(t, x_2) &= v_3(t, x_2) \end{aligned} \tag{3.3}$$

and the continuity of torque

$$\begin{aligned} &2\pi h R^2 G v_{1,x}(t, x_1) = 2\pi h R^2 G v_{2,x}(t, x_1) + 2\pi h_d R_d^2 G_d v_{d,x}(t, x_1) \\ &v_{1,x}(t, x_2) = v_{2,x}(t, x_2) \end{aligned} \tag{3.4}$$

In the second configuration, the continuity equation of displacement $(3.3)_2$ is substituted by the the free end condition

$$v_{d,x}(t, x_1) = 0 \tag{3.5}$$

and the continuity equation of torque $(3.4)_1$ has the simpler form

$$v_{1,x}(t, x_1) = v_{2,x}(t, x_1) \tag{3.6}$$

The right-hand end of the damper in both the configurations is free, as the torque transmitted by sealing is equal to zero

$$v_{d,x}(t, x_2) = 0 \tag{3.7}$$

Therefore, in both the configurations we have eight analytical equations in order to determine the integration constants.

4. Steady-state solution

Assuming a harmonic single frequency excitation ω at the end $x = 0$, steady-state responses of Eqs (2.1) and (2.3) are sought as harmonics with the same angular velocity. For the closed shell, the modal displacements are harmonic in the circumferential direction

$$\begin{bmatrix} v_1(x,t) \\ v_2(x,t) \\ v_3(x,t) \\ v_d(x,t) \end{bmatrix} = \mathrm{e}^{\mathrm{i}\omega t} \begin{bmatrix} V_1(x) \\ V_2(x) \\ V_3(x) \\ V_d(x) \end{bmatrix} \tag{4.1}$$

Substituting we obtain the following system of ordinary differential equations

$$\begin{aligned}
&\rho h\omega^2 V_1 + Gh(1+\beta^2)\frac{d^2V_1}{dx^2} = 0 && 0 < x < x_1\\
&\rho h\omega^2 V_2 + Gh(1+\beta^2)\frac{d^2V_2}{dx^2} - \frac{K}{\delta}(V_2 - V_d) = 0 && x_1 < x < x_2\\
&\rho h\omega^2 V_3 + Gh(1+\beta^2)\frac{d^2V_3}{dx^2} - \frac{K}{\delta}(V_d - V_2) = 0 && x_1 < x < x_2\\
&\rho_d h_d\omega^2 V_d + G_d h_d(1+\beta_d^2)\frac{d^2V_d}{dx^2} = 0 && x_2 < x < \ell
\end{aligned} \tag{4.2}$$

The boundary conditions are obtained from Eqs (3.1)-(3.4) and Eq (3.7) for the first configuration in the following form

$$\begin{aligned}
&V_1(0) = \frac{M_0}{2\pi}hR^2G && V_3(\ell) = 0\\
&V_1(x_1) = V_2(x_1) && V_2(x_1) = V_d(x_1)\\
&GhR^2\frac{dV_1}{dx}(x_1) = GhR^2\frac{dV_2}{dx}(x_1) + G_d h_d R_d^2\frac{dV_d}{dx}(x_1) &&\\
&V_2(x_2) = V_3(x_2) &&\\
&\frac{dV_2}{dx}(x_2) = \frac{dV_3}{dx}(x_2) && \frac{dV_d}{dx}(x_2) = 0
\end{aligned} \tag{4.3}$$

In the second configuration, Eq. $(4.3)_5$ and Eq. $(4.3)_4$ are replaced by

$$\frac{dV_1}{dx}(x_1) = \frac{dV_2}{dx}(x_1) \qquad \frac{dV_d}{dx}(x_1) = 0 \tag{4.4}$$

respectively.

Using the Euler method, solutions in the first and the third section are as follows

$$V_1 = C_1 e^{k_1 x} + C_2 e^{k_1 x} \qquad V_3 = C_7 e^{k_1 x} + C_8 e^{-k_1 x} \tag{4.5}$$

where

$$k_1 = \mathrm{i}\omega\sqrt{\frac{\rho}{G(1+\beta^2)}}$$

In the second section

$$V_2 = \sum_{n=3}^{6} C_n \alpha(k_n, \omega) e^{k_n x} \qquad V_d = \sum_{n=3}^{6} C_n e^{k_n x} \tag{4.6}$$

where

$$\alpha = 1 - \frac{\rho_d h_d \delta}{K}\omega^2 - \frac{G_d h_d (1+\beta^2)\delta}{K} k_n^2$$

the wave numbers k_3, k_4, k_5, k_6 satisfy the following biquadratic equation

$$\begin{aligned} & k^4 G h (1+\beta^2) G_d h_d (1+\beta_d^2) + \\ & + k^2 \Big[G h (1+\beta^2) \Big(\rho_d h_d \omega^2 - \frac{K}{\delta} \Big) G_d h_d (1+\beta_d^2) \Big(\rho h \omega^2 - \frac{K}{\delta} \Big) \Big] + \\ & - \frac{K}{\delta} \Big(\rho h + \rho_d h_d \Big) \omega^2 + \rho h \rho_d h_d \omega^4 = 0 \end{aligned} \tag{4.7}$$

5. Results

The eight unknown coefficients $C_1, C_2, ..., C_8$ are determined by the boundary and the joint conditions described by Eqs (4.3) for the first fixed-free damper configuration, and by Eqs $(4.3)_{1,2,3}$ and Eqs $(4.3)_{6,7,8}$ and (4.4) for the second free-free configuration. Numerical calculations based on the formulas presented in the previous section are performed for a wide range of angular frequency and $M_0/2\pi h R^2 G = 0.001$. More precisely, $\omega = 1\,\mathrm{s}^{-1}$ for the quasistatic loading, in the first shell resonanse, and for a high frequency $\omega = 18250\,\mathrm{s}^{-1}$. The dimensions of the steel cylindrical shell are: $\ell = 0.7\,\mathrm{m}$, $R = 0.062\,\mathrm{m}$, $h = 0.001\,\mathrm{mm}$, $\rho = 7800\,\mathrm{kg/m}^3$. The Kirchhoff modulus is equal to $G = 80\,\mathrm{GPa}$. The rheological property of steel is described by the Voigt-Kelvin model with a retardation time $\lambda = 0.001\,\mathrm{s}^{-1}$. The electrorheological fluid-filled damper is located between $x_1 = 0.25\,\mathrm{m}$ and $x_2 = 0.55\,\mathrm{m}$. The inner shell is also made of steel with the thickness $h_d = 0.001\,\mathrm{m}$.

The gap thickness is equal to $\delta = 0.001\,\mathrm{m}$. The data of electrorheological fluid (Lord Corporation VersaFlo III ER) are given by Yalcintas and Coulter (1995). In calculations, the quadratic dependence of the storage modulus of ERF on the applied electric field is assumed kV/mm. The loss modulus is found to be almost constant and quite small in magnitude. Calculations are performed for the following values of voltage applied to ER material $U = 0$, 1, 2, 3, 3.5 kV. In Fig. 3 ÷ Fig. 10 the results of calculations are given. The circumferential vibration amplitude of the shell in the first configuration as a function of angular velocity for electrical fields of 0, 1, 2, 3, and 3.5 kV is plotted in Fig. 3. The circumferential vibration response is calculated at the place of torque excitation $x = 0$. In the figure, the peak values of each curve represent the resonanse frequencies of the shell.

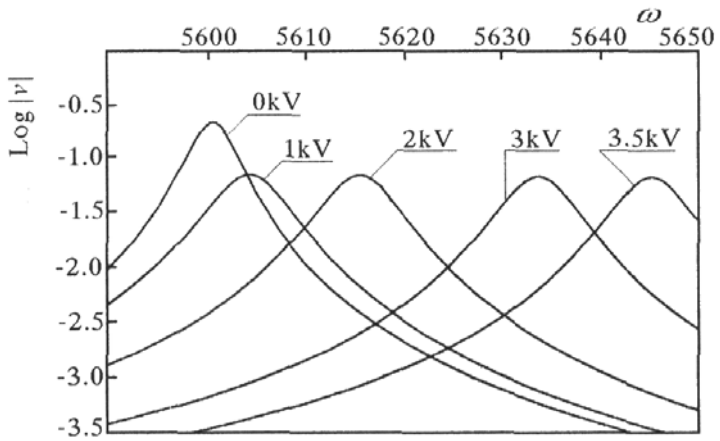

Fig. 3. Near-field shell circumferential response v_1 at $x = 0\,\mathrm{m}$ – the first configuration

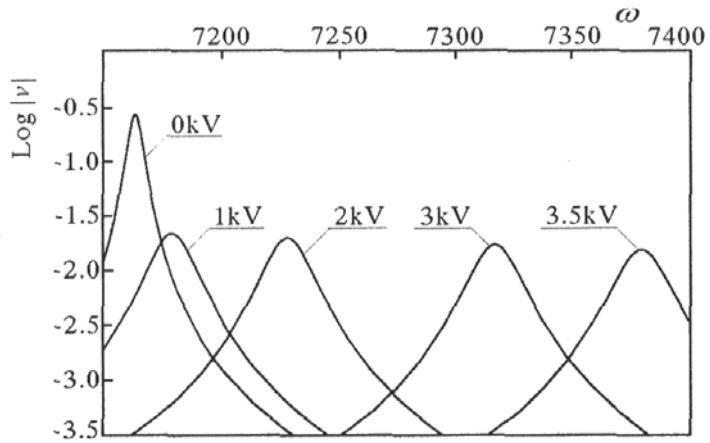

Fig. 4. Near field shell circumferential response v_1 at $x = 04\,\mathrm{m}$ – the second configuration

As the electric field increases, the resonanse frequencies shift to higher values while the circumferential modal response of the structure is decreased. Figure 4 illustrates a similar trend of the shell in the second configuration with the free-free damper. Due to the simpler mechanical structure, the resonanses are shifted to higher values in comparison with the first configuration of the fixed-free damper. From the figure, a greater damping effectiveness of this configuration can be seen.

Considering both the configurations, the observations can be explained as follows: an increase of the applied field causes an increase in stiffness of the damping layer and an increase of the natural modal angular velocities. The static dependence ($\omega = 1\,\mathrm{s}^{-1}$) of the main shell and fixed-free damper on

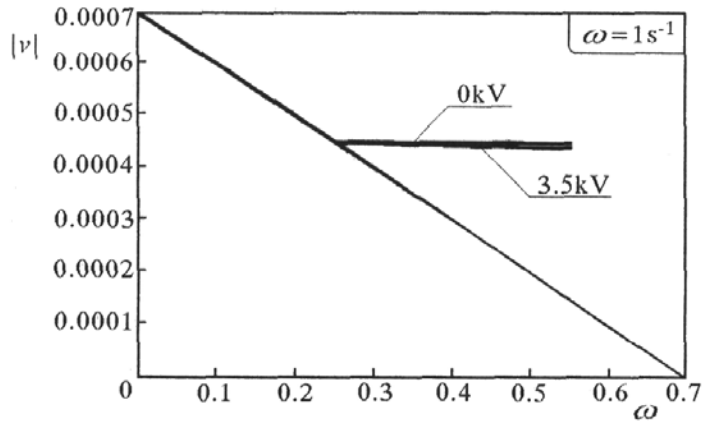

Fig. 5. Shell and fixed-free damper circumferential displacement distribution at $\omega = 1\,\mathrm{s}^{-1}$ – the first configuration

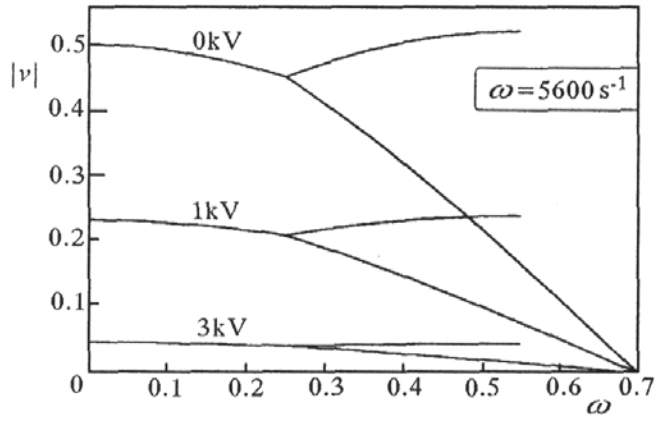

Fig. 6. Shell and fixed-free damper circumferential displacement distribution at $\omega = 5600\,\mathrm{s}^{-1}$ – the first configuration

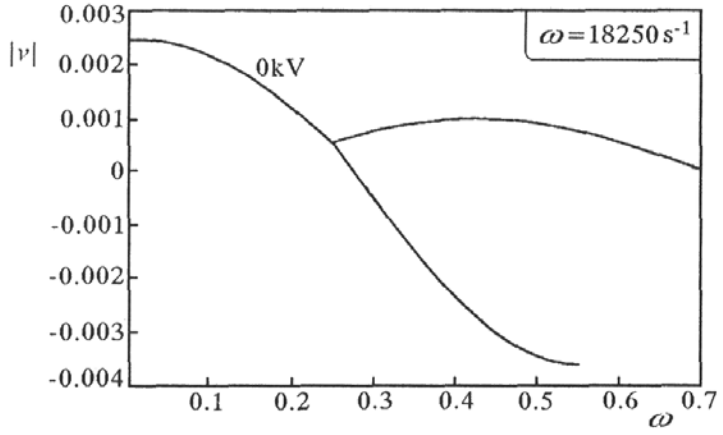

Fig. 7. Shell and fixed-free damper circumferential displacement distribution at $\omega = 18250\,\mathrm{s}^{-1}$ – the first configuration

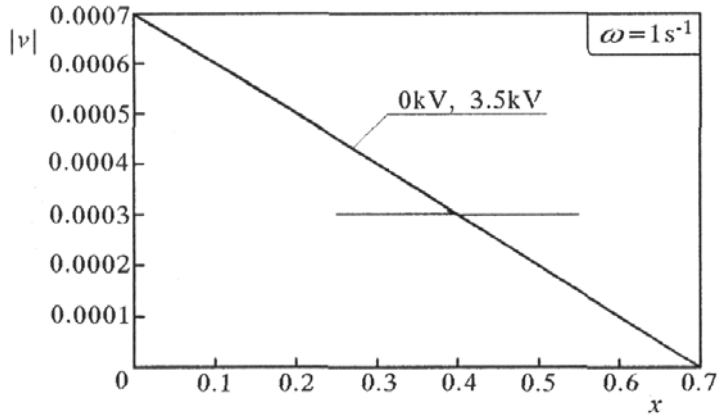

Fig. 8. Shell and free-free damper circumferential displacement distribution at $\omega = 1\,\mathrm{s}^{-1}$ – the second configuration

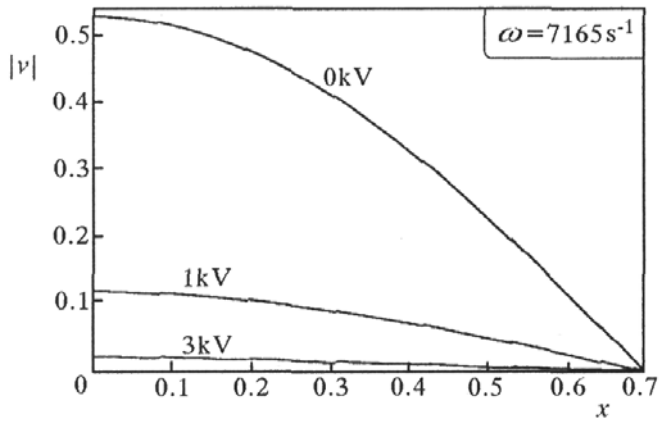

Fig. 9. Shell and free-free damper circumferential displacement distribution at $\omega = 7165\,\mathrm{s}^{-1}$ – the second configuration

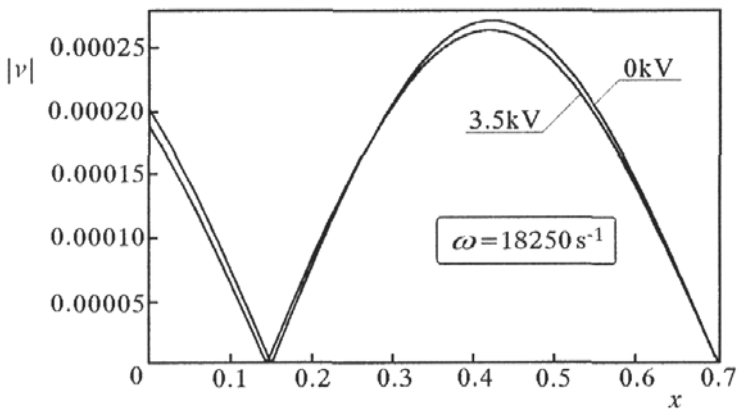

Fig. 10. Shell and free-free damper circumferential displacement distribution at $\omega = 18250\,\mathrm{s}^{-1}$ – the second configuration

the position x for different values of the applied field is shown in Fig. 5. As expected, due to a slow change of applied electric field, the space distribution of cicrumferential shell displacement is insignificantly affected by the field. The displacement of the damper is almost constant.

Fig. 6 presents the shell and damper circumferential displacements at the resonanse $\omega = 5600\,\mathrm{s}^{-1}$. The electrical field decreases significantly the amplitude of torsional vibrations. The amplitude of damper vibrations is not uniformly distributed over the range x_1, x_2. Fig. 7 shows the spatial distribution of vibration amplitude at the high angular frequency $\omega = 18250\,\mathrm{s}^{-1}$. The shell and the damper displacement have opposite directions.

The spatial distributions of main shell and damper displacements in the second free-free configurations have different shapes (Fig. 8, Fig. 9, and Fig. 10). The damper essentially is not deformed, but due to a large relative motion between the shell and the damper, the damping effectiveness is greater in comparison to the first configurations.

At a high angular velocity region, the influence of electric activation on the vibration amplitude is much smaller than in the resonanse range. The amplitude of damper displacement is almost equal to zero (Fig. 10).

6. Conclusions

A dynamic model has been developed which is able to predict the forced torsional response of a shell in the presence of ER damper mounted on the main shell in the middle section. The damper driven by an electrical field in the radial direction is used to decrease the amplitude of torsional vibration. Two different configurations are examined: in the first one, the fixed-free boundary conditions are imposed on the damper shell, in the second configuration the damper satisfies the free-free boundary conditions. Calculations performed for steady-state harmonic vibrations of the shell confirm damping effectiveness of both configurations. Nevertheless, in the second configuration the damping effectiveness is more pronounced. Frequency characteristics of near field shell and spatial distributions of shell and damper for the different driving frequencies are shown.

Acknowledgment

This research has been supported by the State Committee for Scientific Research, Warsaw, Poland, under grant BS 504 G 1152 0818 001.

References

1. SHIANG A.H., COULTER J.P., 1996, A comparative study of AC and DC electrorheological material based adaptive structures in small amplitude vibration, *Journal of Intelligent Material Systems and Structures*, **7**, 455-469

2. CHOI Y., SPRECHER A.F., CONRAD H., 1992, Response of electrorheological fluid-folled laminate composites to forced vibration, *Journal of Intelligent Material Systems and Structures*, **3**, 17-29

3. ROSS D. ET AL., 1959, Damping of plate flexural vibrations by means of viscoelastic laminate, *Structural Damping*, ASME, 49-88

4. MEAD D.J., MARKUS S., 1969, The forced vibrations of a three-layer damping sandwich beam with arbitrary boundary conditions, *Journal of Sound and Vibration*, **10**, 163-175

5. TYLIKOWSKI A., 2000, Dynamic stability of electrorheological fluid-filled laminate, *Journal of Theoretical and Applied Mechanics*, **38**, 417-428

6. OLDROYD J.G., 1953, The elastic and viscotic properties of emulsions and suspensions, *Proceedings of the Royal Society of London*, **A218**, 122-132

7. HAN SU JEON., 1999, A study on stress and vibration analysis of a steel and hybrid flexpline for harmonic drive, *Composite Structures*, **47**, 827-833

8. OSTAPSKI W., 1998, Engineering design of harmonic drive gearings towards quality criteria, *Machine Dynamics Problems*, Warsaw University of Technology, **21**, 54-99

9. YALCINTAS M., COULTER J.P., 1995, Analytical modeling of electrorheological material based adaptive beams, *Journal of Intelligent Material Systems and Structures*, **6**, 488-497

10. YALCINTAS M., DAI H., 1999, Magnetorheological and electrorheological materials in adaptive structures and their performance comparison, *Smart Materials and Structures*, **8**, 560-573

Modelowanie adaptacyjnych powłok z cieczą elektroreologiczną

Streszczenie

Ciecze elektroreologiczne wykazują szybkie zmiany swoich właściwości reologicznych pod wpływem pola elektrycznego. W pracy przedstawiono analizę drgań za-

mkniętej walcowej powłoki częściowo wypełnionej cieczą elektroreologiczną poddaną działaniu pola elektrycznego. Zastosowanie tego rozłożonego tłumika semiaktywnego powoduje zmniejszenie drgań skrętnych powłoki jako części przekładni falowej w porównaniu z klasycznym rozwiązaniem. Zbadano dwie konfiguracje tłumika i stwierdzono, że tłumik pływający ma lepsze właściwości tłumiące w porównaniu z tłumikiem jednostronnie sztywno połączonej z powłoką.

Manuscript received March 13, 2002; accepted for print April 3, 2002